International Journal of Microwave and Wireless Technologies, 2017, 9(5), 1045–1057.
doi:10.1017/S1759078716001045

RESEARCH PAPER

A new efficient and proper modeling of isotropic/uniaxial anisotropic substrate specifications in design procedures of metasurfaces

SARA MOINZAD[1], ALI ABDOLALI[1] AND BAGHER NOORBAKHSH[2]

Specifications of the substrates are among the most important and problematic parameters that still do not have proper models in the design procedures of metasurfaces. In this paper, a new fast and exact algorithm based on artificial neural networks (ANNs) is presented, which makes it possible to design frequency-selective surfaces (FSSs) on various kinds of standard substrates. Also for the first time, designing FSSs on uniaxial anisotropic substrates can be easily done in short time and without any optimization algorithms. During this paper, first equivalent geometry approach (EGA) is demonstrated as a new method of preparation the ANNs. Then EGA is used to train geometry transformation ANNs. The advantage of this approach is to reduce the size of training datasets by about 98% and prevent from superfluous simulations. Hence, the time needed for training of the networks is much less than before. Numerical results are used to show that the required time for developing FSSs is <200 ms on average, and errors are <2%. For the final validation, a prototype sample of FSS is fabricated on the RO4003 substrate with 20 mil thickness. Both analytical and experimental results confirm the correctness of the predicted values.

Keyword: Frequency selective surfaces, Artificial neural networks, Uniaxial substrates, Periodic substrates, Liquid crystal substrates

Received 26 September 2015; Revised 5 August 2016; Accepted 9 August 2016; first published online 14 November 2016

I. INTRODUCTION

Frequency-selective surfaces (FSSs) are widely used for the synthesis of complex electromagnetic media such as metamaterials, metaferrites, artificial magnetic conductors, and absorbers [1–4]. These structures are the arrays that usually consist of metallodielectric patches or apertures supported by a dielectric substrate and superstrate [5, 6]. In recent years, FSSs are employed also for the synthesis of microwave devices such as filters, radomes, polarizers, reflectarrays, and so on [7–11]. Because of the applicability of FSSs, the methods that are used in designing these structures become important. These methods must have enough accuracy and universality to be able to cover all of the applications. One of the most important steps in the design procedure is the specification/selection of substrates. In general, substrate manufacturers determine specifications of the substrates, and then designers have to choose one of these standard substrates after paying attention to the requirements of the project, project budget, and ease of accessibility. Hence, the design procedure must be flexible in terms of their choice, and the substrate specifications should be removed from the optimization parameters.

On the other hand, in some cases, the complex substrate needs to be defined by users to satisfy the requirements of the desired special application, such as liquid crystal substrates with anisotropic permittivity, biased ferrites with anisotropic permeability, and periodic substrate with equivalent anisotropic permittivity. Therefore, in the design procedure, the substrate specifications should be devolved to the designer as the input parameter. Such a goal first needs the accurate numerical modelization of the effects of substrate specifications on the frequency response of FSSs. This modelization should be considered such that it could directly design the FSS on any substrate without any optimization algorithms.

In the past few decades, many methods have been investigated for calculating the scattering parameters of FSSs with various kinds of substrates and analyzing the effect of the substrate specifications on the resonance frequency of FSSs. The influence of changes in the thickness of substrates was investigated in [12], showing that for the thicknesses of smaller than 5 mm, with increasing the thickness of dielectrics, the resonance frequency was reduced. Also in [13], it was found that, with increasing permittivity of the substrate, the resonance frequency was reduced.

Furthermore, in recent years, because of the growing interest in the field of complex electromagnetic media, the analysis

[1]Applied Electromagnetics Laboratory, Iran University of Science and Technology (IUST), Narmak, Tehran 1684613114, Iran
[2]Faculty of Electrical Engineering, K. N. Toosi University of Technology, Tehran, Iran
Corresponding author:
S. Moinzad
Email: smoinzad@elec.iust.ac.ir

of FSSs with anisotropic substrates has been studied more. Scattering parameters of FSSs with uniaxially and biaxially anisotropic substrates have been calculated in [14–20] using moment method with immittance approach or Galerkin's method in combination with the equivalent transmission line. Also qualitative studies have been done on the effect of anisotropy and variation in the elements of permittivity tensor on the frequency response of FSSs.

As can be seen in [14–20], although many methods have been studied for FSS analysis with these complex substrates, designing FSSs with these substrates is an unsolved problem yet.

The aim of this paper is to present a design procedure that is flexible with respect to the changes in the substrate specifications. This design process is based on the new artificial neural networks (ANNs) called geometry transformation ANNs (GTANNs). As a result, the substrate specifications must be considered in the design procedure, but be removed from the inputs/outputs of ANNs. So, GTANNs are trained to transform the responses of main ANNs, proportional to the selected dielectric as a substrate. With this approach, the flexibility of the design algorithm is improved, and at the same time, prevents from increase in the required presimulations. The presented design algorithm can design the FSSs on any standard substrate quickly and precisely. In addition, the purpose of the effort in this paper is to show that this approach not only can cover the all of the standard substrates, but also can be the beginning step for developing the algorithms that directly design FSSs on the complex substrates. It is shown that designing FSSs on complex substrates first needs an appropriate model that can design FSSs on simple standard substrates. Using this model and some approximated formulas, FSSs can be developed on any other complex substrates. So the last section of the paper is dedicated to designing FSSs on the uniaxial substrates that are the best examples for showing the above issue, *because many complex substrates, such as periodic substrates or liquid crystal substrates are considered as uniaxial substrates*.

The organization of this paper is as follows: In Section 2, the modelization and design of FSSs with the standard substrates are qualitatively and numerically studied, and GTANNs are demonstrated. Afterwards, the experimental results are discussed to show the correctness of GTANNs in Section 3. Then, in Section 4 based on the results of Section 2, the suitable design algorithm for uniaxially anisotropic substrates is presented.

II. MODELING FSS WITH STANDARD SUBSTRATES

Even now, the most popular technology that is used to fabricate the FSS structures is the printed circuit board (PCB). In PCB technology, high-frequency substrates have standard permittivities and thicknesses, which are determined by the manufacturers such as Rogers Corporation, Taconic Corporation, etc. Based on the published datasheets, the typical values of permittivities (ε_r) are between 1.5 and 12.5. Also thicknesses (h) are within the range of 5–125 mil. Variations in the specifications of the substrate have a strong effect on the frequency response of FSSs, which could not be disregarded or easily taken into account. Hence, it is important for these effects to be considered in design procedures by suitable methods.

Equivalent circuit models (ECM) are the most commonly used ones for designing FSSs. With ECM, the approximate analytical formulas for designing square loops are provided by Marcuwitz, Langley, and Lee [21–23]. These formulas contain the geometric dimensions of square loops as follows:

$$\frac{X}{Z_0} = \frac{L}{P_1} F(P_1.2w_1.\lambda) = \frac{P_1 \cos\theta}{\lambda}\left[\ln\left(\csc\left(\frac{P_1 w_1}{2\pi}\right)\right) + G(P_1.2w_1.\lambda.\theta)\right], \quad (1)$$

$$\frac{B}{Z_0} = 4\frac{L}{P_1} F(P_1.P_1 - L.\lambda), \quad (2)$$

$$G(P_1.2w_1.\lambda.\theta) = \frac{0.5(1-\beta^2)^2[(1-\beta^2/4)(A_{1+}+A_{1-})+4\beta^2 A_{1+}A_{1-}]}{(1-\beta^2/4)+\beta^2(1+\beta^2/2-\beta^4/8)(A_{1+}+A_{1-})+2\beta^6 A_{1+}A_{1-}}, \quad (3)$$

$$A_{1\pm} = \frac{1}{\sqrt{(P_1 \sin\theta/\lambda \pm 1)^2 - P_1^2/\lambda^2}} - 1, \quad (4)$$

$$\beta = \sin\left(\frac{0.5\pi w_1}{P_1}\right), \quad (5)$$

where X is the equivalent inductance and B is the equivalent capacitance of the structure, P_1 is a period of structure, w_1 is the width of strips, L is the outer side of the square loop, θ is the angle of incidence, Z_0 is free space impedance, and λ is the free space wavelength. All of these parameters are shown in Fig. 1(a). As can be seen, ε_r and h have not been directly considered in (1)–(5). In few cases, the permittivity effect on resonance frequency (f_r) is considered a scale factor, as defined in (6) or (7).

$$f_{r1} = \frac{f_{ro}}{\sqrt{1+\varepsilon_r/2}}, \quad (6)$$

$$f_{r2} = \frac{f_{ro}}{\sqrt{\varepsilon_r}}, \quad (7)$$

where f_{ro} is the resonance frequency of freestanding FSS, f_{r1} is the resonance frequency of FSS with the substrate, f_{r2} is the resonance frequency of sandwiched FSS between dielectrics and ε_r is the relative permittivity [24]. Although these scale factors have excellent accuracy, they are limited to the resonance frequency and cannot be applied to other frequency bands or other parameters, such as the phase of scattering parameters or surface impedance. In some works, such as designing filters and radomes, resonance frequency is operational frequency as well. So, modeling resonance frequency is enough in these cases, but in some other works such as designing flat microwave lenses or reflectarray antennas, users need to know the phase of S-parameters in all the band pass regions of the structure. By modeling the resonance frequency, only zero phase point is modeled and position of the other phases is unknown for the user. In addition, these formulas cannot design FSSs by themselves standalone and

https://doi.org/10.1017/S1759078716001045 Published online by Cambridge University Press

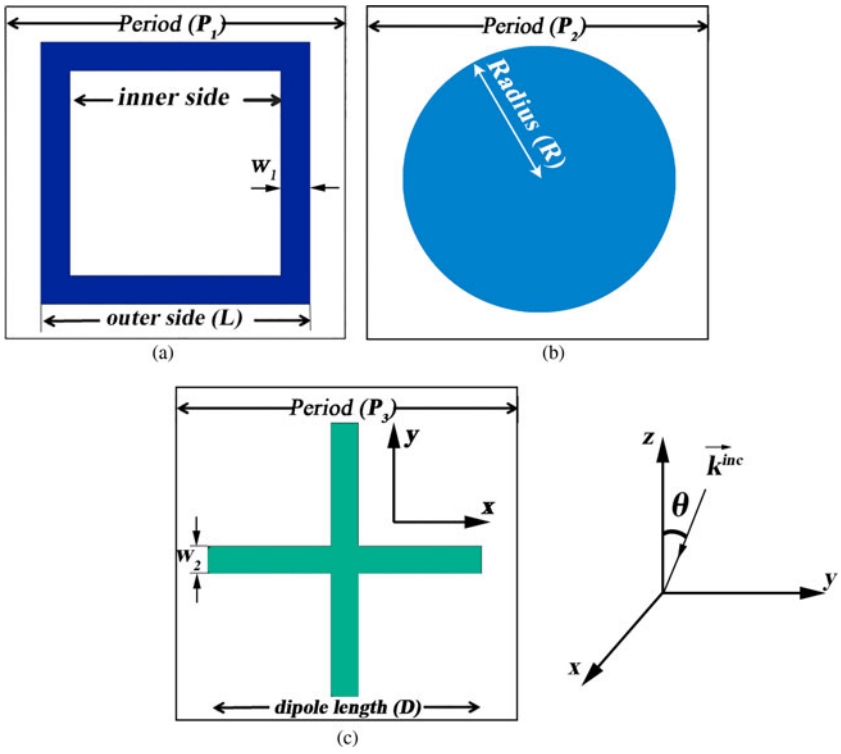

Fig. 1. Proposed structures: (a) square loop, $W_1 = 0.4$ mm, $P_1 = L + 0.8$ mm; (b) circular patch, $P_2 = R + 0.8$ mm; (c) crossed dipoles, $W_2 = 0.8$ mm, $P_3 = D + 0.8$ mm.

optimization algorithms should accompany these formulas. So, scale factors are not suitable for modeling the structure.

One of the other most popular methods for designing FSSs is ANN-based models, which consist of layers built by nonlinear functions and act like biological neurons. So, ANNs are powerful tools for modeling nonlinear multi-input multi-output systems, such as FSSs. In recent years, many methods have been investigated for designing FSSs based on ANNs. Although these methods are better than approximate formulas, they do not have enough efficiency and the design procedures have still some deficiencies. In this work, ANN-based models are chosen owing to their speed and accuracy.

In recent works, ANNs have been only used as a response calculator unit, which calculate the frequency response of FSSs with the input of geometric dimensions. So, FSS design procedures consisting of these networks must be accompanied by the suitable optimization algorithm and desired convergence conditions. Three methods exist by which substrate specifications can be considered in the ANN-based design procedures:

(1) Both ε_r and h are assumed to be constant.
(2) Both ε_r and h are the direct input of ANNs, like other geometric dimensions [24–27].
(3) Neither ε_r nor h is the direct input/output of ANNs, but ANNs can transform geometric dimensions in proportion to the chosen substrate.

The first method is suitable for the special cases, in which ε_r and h are determinate, but in general-purpose algorithms this method may not support all of the applications. In the second method, the specifications of the substrate are inputs of the ANNs. Hence, in the design algorithm, ε_r, and h are the output parameters determined by optimization algorithms. Problems that are produced using this method are first the fabrication facility of the structures, because the substrate specifications resulted by the optimization procedure might not exist as a standard substrate. The second problem is the large size of training datasets. For example, in [25], both ε_r and h were the inputs of ANNs. So, with six samples of ε_r and six samples of h, the total size of training dataset was 5400 samples. In addition, in [26, 27], sizes of the training datasets were 5832 and 198 samples, respectively. Unlike the first and second methods that have been investigated in most of the previous works, the third method is an optimum method that is suggested in this paper for the first time. In the third method, the substrate specifications are the input of the design algorithm, instead of the input of ANNs, and optimization algorithms are not used. So, ε_r and h can be determined by users. Also 5400, 5832, and 198 samples in previous works can be reduced to only 260, 520, and 60 samples, respectively, and the cost that must be paid for large datasets is eliminated.

At last, it is desired to comprise the CST/HFSS optimizers with the proposed method. Let us assume that it is desired to design flat lens in X-band region. This lens has dimensions about 160×130 mm^2 consisted of unit cells with periodicity of 8 mm on average. So approximately 280 unit cells exist and optimization procedure must be repeated 280 times to design this flat lens; also, for each optimization it is assumed that 30 iterations are needed at least [25] to achieve the desired phase. The total number of the simulations is 4160 (280×30). Whereas it will be shown in this paper for training the GEANNs, with frequency step by about 0.5 GHz, and phase step by about the 10°, 396 samples are required. In addition, for training the GTANNs 189 samples needed to cover all of the substrates. So, the total number of the pre-simulations in this case is only 585 samples ($189 + 396$). Hence, the required simulations are reduced to about 85.93%.

https://doi.org/10.1017/S1759078716001045 Published online by Cambridge University Press

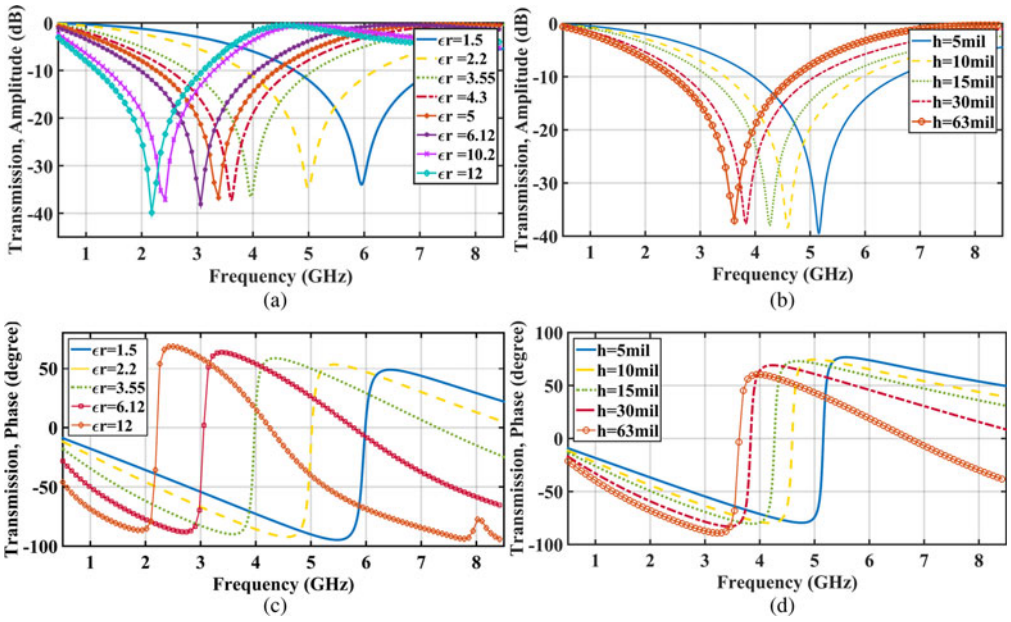

Fig. 2. Changes of frequency responses of the square loop due to the changing of substrate permittivity and thickness (a) $|S_{12}|$, (b) $|S_{12}|$, (c) $<S_{12}$, (d) $<S_{12}$.

This section is followed by the subsections, which include the manner of changing frequency response of FSSs as result of changing the substrate specifications and describe the best solution for its modeling.

A) Equivalent geometry approach (EGA)

Nowadays, various types of substrates with different specific applications are used in industrial designs. Temperature, humidity, flexibility, and many other parameters are involved in the selection of the suitable substrate. Accordingly, the effect of substrate specifications on the frequency response of FSS has been studied in many works such as [12–20]. In previous studies, the manner of changing frequency response has been described as frequency scaling and changing the substrate compressing or expanding the frequency response of FSSs.

It is obvious that, in frequency scaling manner, scale factors depend on frequency, geometric dimensions, angle of incidence, polarization of incident wave, etc. However, these dependencies are not considered in the scale factors presented in previous works and used in (1) and (2). Similar approximations can produce significant errors in design procedures. Totally, deficiencies of frequency scaling theorem generate the need for further studying and completion of the details of this theory.

For better understanding, consider the square loop as in Fig. 1(a). This square loop has an outer side of L, the period that is 0.8 mm bigger than L, the inner side that is 0.8 mm smaller than L, and the FR4 substrate with 63 mil thickness and permittivity of about 4.3. The proposed square loop is simulated using various other kinds of substrates and the responses are presented in Fig. 2. As can be seen, although the replies have frequency scaling, domains, especially the domain of phases, are also scaled. In other words, changes of substrate result in changing the bounds of the amplitude/phase of scattering parameters. For example, in Fig. 2, the maximum phase of transmission varies from 60° to 76°. Hence, it cannot precisely determine which point on the reference response is scaled to which points on the other responses. In addition, some points may not have an equivalent point on the secondary responses. Hence, the exact determination of scale factors is impossible.

On the other hand, the scale factors can only be used for FSSs analysis and design of structures needs the application of the optimization algorithms. As a result of these drawbacks, the frequency scaling theorem is not an efficient solution for modeling the effect of substrate on the frequency responses of FSSs. For a better solution, it needs a closer look at the efficacious parameters for the answer of FSSs. If the manner of changing in response due to the changing in the substrate is the same as the one for these parameters, then it is possible to employ this parameter to compensate for the changes of responses.

It means that, with changing this parameter, the response must return to the first state. Studies on parameters have revealed that the effective parameters that can compensate for the changes of frequency responses are geometric dimensions. Hence, this method is called EGA. For further investigation of EGA, the three unit cells with different kinds of geometry shown in Fig. 1 are simulated. Simulation results that are depicted in Fig. 3 affirm that, for changing ε_r, the amplitude and phase of scattering parameters can be completely compensated for and be congruent to the reference response by changing the geometric dimensions.

Figure 3 also depicts that altering the shape of the FSS from the square loop to circular patch and crossed dipoles cannot reject EGA. This principle remains true for changing thickness, except the phase of the scattering parameters.

To model the phase differences between the main and equivalent structures, first, assume a plane wave with propagation along the + z-direction.

Once this wave passes through the square loop FSS with $L = L_1$, $h = h_1$, and $\varepsilon_r = \varepsilon_1$, this structure can be modeled as a two-port network and have the scattering parameters of $S^{(1)}$. In the next step, the height of the substrate is changed. Following that, the outer side of the square loop is also changed to compensate for the frequency response changes.

https://doi.org/10.1017/S1759078716001045 Published online by Cambridge University Press

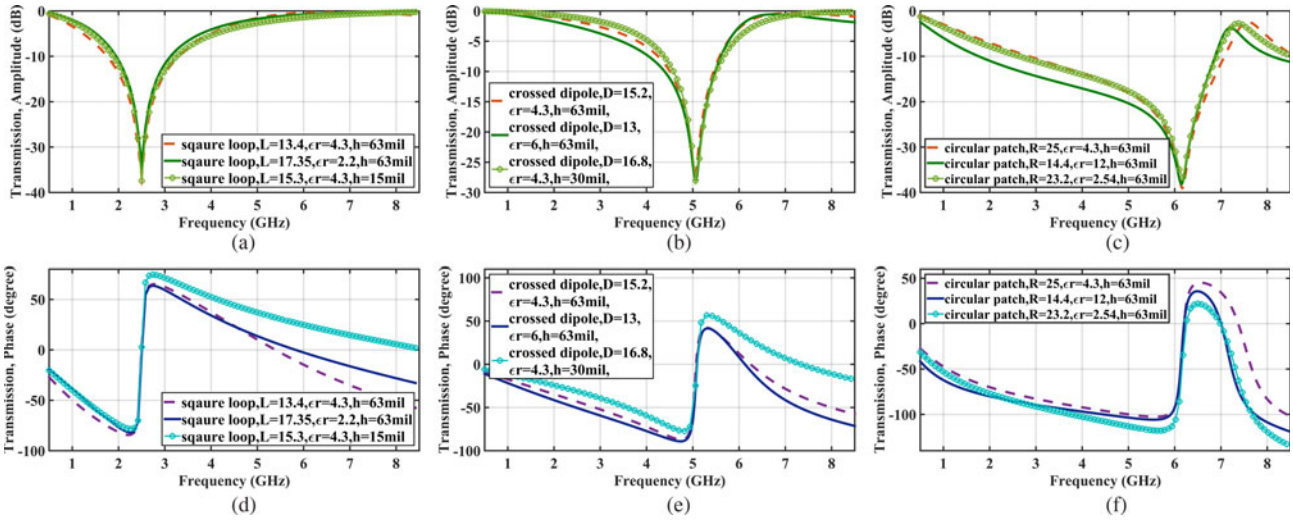

Fig. 3. Frequency responses of square loop, circular patch and crossed dipoles that have different geometric dimensions and different substrate specifications but have same frequency response (a), (b), (c) $|S_{12}|$, (d), (e), (f) $<S_{12}$.

Hence, the wave passes through the square loop FSS with $L = L_2$, $h = h_2$, and $\varepsilon_r = \varepsilon_1$. The amplitude of frequency response is equal to previous case and only their phases are different (all of the S-parameters such as reflections and transmissions, have same differences in these two cases). According to the simulations, it can be seen that this difference is a function of frequency, first dimension of the square loop (L_1), permittivity, and thickness of substrate.

$$\left|S^{(2)}\right| = \left|S^{(1)}\right|, \tag{8}$$

$$\measuredangle S^{(2)} = \measuredangle S^{(1)} + \Delta(\varepsilon_r.L_1.\Delta h.f), \tag{9}$$

$$\Delta h = h_2 - h_1. \tag{10}$$

For simply modeling this relation, it is assumed that

$$\Delta(\varepsilon_r.L_1.\Delta h.f) = \beta_m(\varepsilon_r.L_1.f) \times \Delta h, \tag{11}$$

where β_M is propagation constant of wave in metalodielectric FSS, h_1 is the thickness of reference substrate, and h_2 is the thickness of the secondary substrate. Hence, the phase differentiation can be easily taken into account in the design procedure. It is sufficient to determine β_M versus frequency using one of the thicknesses and, then, $\Delta\varphi$ can be easily calculated for every Δh. Although this formulation does not completely match the reality of wave propagation in this structure, it is the simplest method for modeling the phase differences. For better illustration, L_1 is set to 13.4 mm and values of L_2 are determined for eight samples of ε_r ([1.5, 2.2, 3.55, 4.3, 5, 6.12, 10.2, and 12]). Then, differences between the responses are calculated and values of β_m in Fig. 4 are estimated. By the end of this step, there is no estimation that could produce the error in Fig. 4. For the proposed square loop (Fig. 1(a)), β_M versus frequency is obtained as in Fig. 4 for every kind of dielectrics with the desired ε_r in the range of 2.2–10.2.

The only remaining problem is the determination of the dependency of EGA method on the polarization and angle of incidence. EGA is an independent approach that, despite being applied for the perpendicular incidence of transverse electric (TE) polarization wave, can solve the design problem for both polarizations and any angle of incidence. Figure 5 clearly provides the proof of this principle.

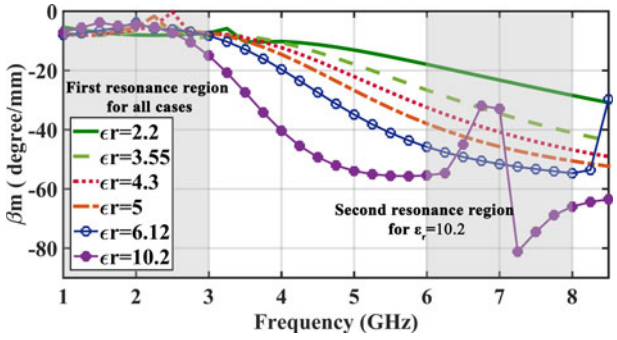

Fig. 4. β_M versus frequency for substrate permittivity between 1.5 and 12, $L_1 = 13.4$ mm.

The equivalent length obtained for TE polarization and perpendicular incidence is suitable for other polarizations and angles of incidence and also the responses are well in congruent. In the next subsection, the utilization of EGA in training GTANNs and designing FSSs is described.

B) Trained networks

According to the previous results, two kinds of networks are needed: one for designing FSS on the reference substrate and another for transforming the dimensions into the input substrate. The configuration of these networks is demonstrated in Fig. 6. Marquardt–Levenberg training algorithm is adopted for all the networks owing to its efficiency and fast convergence. Also mean squared error (MSE) is used as the performance index during the training process. The MSE of an estimator measures the average of the squares of the errors, that is, the difference between the estimator and what is estimated. So MSE is calculated as:

$$\text{MSE} = \frac{1}{n}\sum_{k=1}^{n}(\hat{\varphi}_{S12k} - \varphi_{S12k})^2. \tag{12}$$

https://doi.org/10.1017/S1759078716001045 Published online by Cambridge University Press

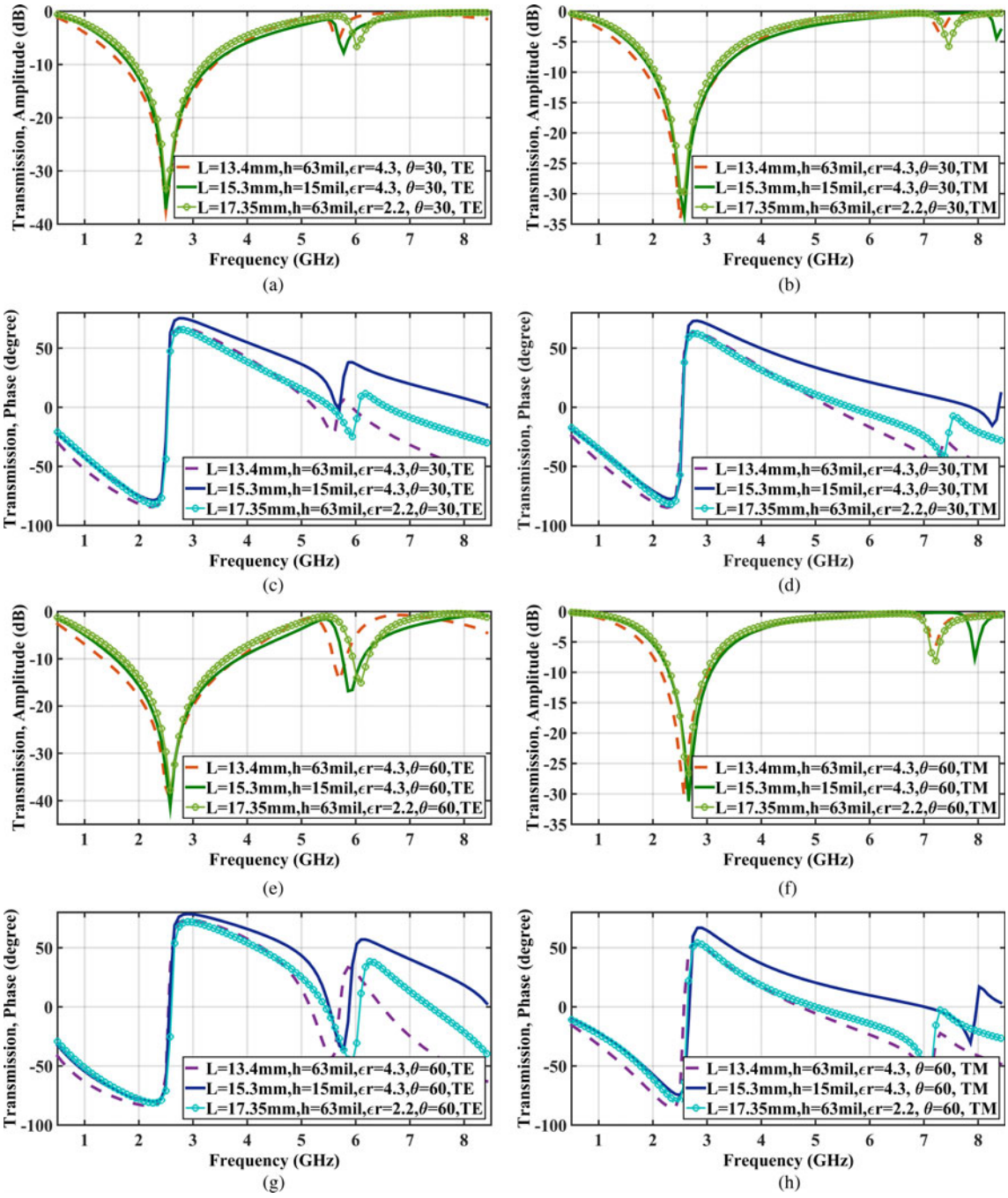

Fig. 5. The frequency response of square loop with a length of L under four different incidence condition. (a) $|S_{12}|$ for TE wave with $\theta = 30^\circ$; (b) $|S_{12}|$ TM wave with $\theta = 30^\circ$; (c) $<S_{12}$ for TE wave with $\theta = 30^\circ$; (d) $<S_{12}$ for TM wave with $\theta = 30^\circ$; (e) $|S_{12}|$ for TE wave with $\theta = 60^\circ$; (f) $|S_{12}|$ for TM wave with $\theta = 60^\circ$; (g) $<S_{12}$ for TE wave with $\theta = 60^\circ$; (h) $<S_{12}$ for TM wave with $\theta = 60^\circ$.

That n is the number of the training samples, $\hat{\varphi}_{S12}^{(k)}$ is output of the network for kth sample and $\varphi_{S12}^{(k)}$ is target value of the kth sample.

For training the first network, 27 samples of L between 4 and 19 mm and seven samples of the angle of incidence (θ) between 0° and 60° are provided. With these values for L frequency bands from 1 to 12 GHz, L, C, S, and X are completely covered. So, the number of the required pre-simulations is 189 (27×7). With the pre-simulation results (amplitude and phase of transmission), a training dataset is obtained and the training process was begun.

Both networks provide the output of L in the mm unit for the FR4 substrate with 63 mil thickness as the reference substrate. If TE polarization is intended, then $P = 1$; otherwise, $P = 2$. The topology of these networks has two hidden layers with four and three nodes, respectively, and a single-node output. The validation MSEs are 1.4017×10^{-5} and 1.9568×10^{-5}.

For training the transforming part, fewer samples of L (about 10%) are needed: [19, 13.3, 7, and 4]. The number of ε_r samples for the third network is 8 ([1.5, 2.2, 3.55, 4.3, 5, 6.12, 10.2, and 12]). Also, network 4 has seven samples of h

https://doi.org/10.1017/S1759078716001045 Published online by Cambridge University Press

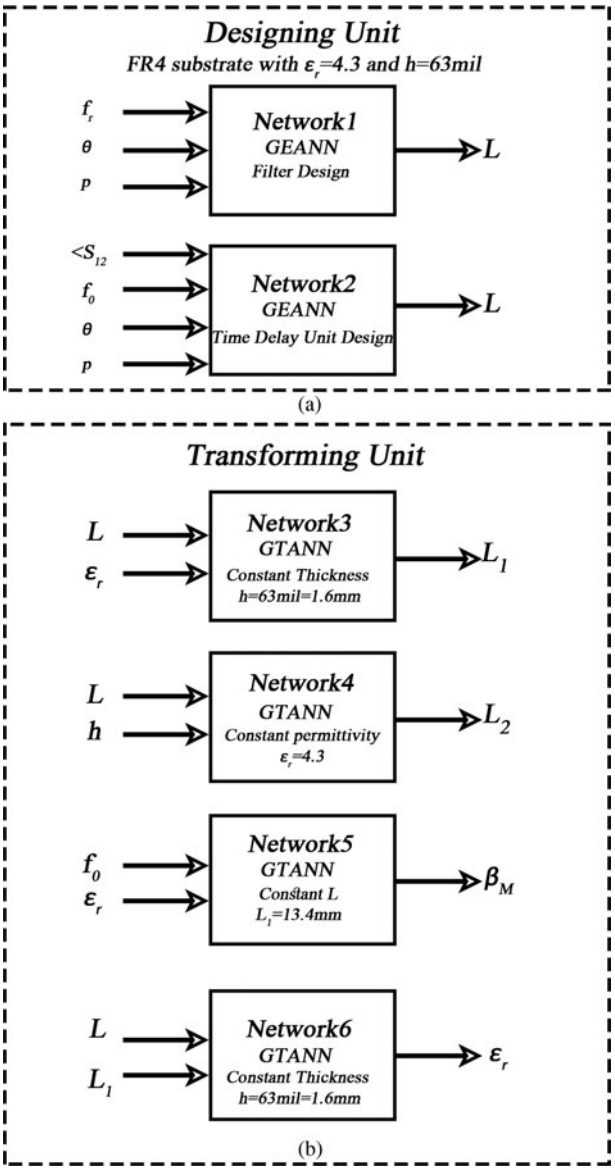

Fig. 6. The configuration of trained networks: (a) designing unit, (b) transforming unit.

([5, 10, 15, 30, 63, 100, and 125]). Hence, the training datasets have 32 and 28 elements for training these networks. It is important that if the substrate specifications are the direct input of main designing networks, the total size of the pre-simulations become 10584 ($27 \times 7 \times 8 \times 7$). However, this huge number of simulations will be reduced to 258 ($189 + 32 + 28$) samples, i.e. 97.5% reduction in the required pre-simulations.

The transforming networks, called GTANNs, are four feed-forward networks the configuration of which is shown in Fig. 6(b). The first networks transform L to compensate for the changes in the permittivity of substrate. This network has the MSE of about 1.9006×10^{-4}, and its thickness is constant. To compensation for the thickness, the second and third networks are trained by the MSEs of about 3.1486×10^{-4} and 3.8209×10^{-3}, respectively. The sixth network is also trained for designing structures on anisotropic substrates. This network is the inverse of the third network and has similar topology and MSE. These networks, except the fifth one, have two nodes in the hidden layer and a single-node output layer. The fifth network also has a hidden layer with 20 nodes and a single-node output layer.

C) Design algorithm

For designing the FSS on the substrate with the desired ε_r and h, an appropriate algorithm that was joined with the trained networks is needed. This algorithm which is shown in Fig. 7 begins by taking the inputs such as $<S_{12}$, f_o/f_r, θ, p, ε_r, and h. If the goal is $<S_{12}$, first β_M, is calculated using f_o and ε_r, and then, $\Delta\varphi$ will be calculated. Value of β_m must be calculated with due attention to L_1, which is no longer equal to 13.4 mm. Based on EGA, we know that the structures shown in Fig. 8 are equivalent. So for achieving the correct value of β_m, we must calculate $\varepsilon_r = \varepsilon$. In fact, ε_r that is used for β_m calculation is different from the input ε_r and determined by network 6 during the iterative section of our algorithm.

Based on the flowchart in Fig. 7, in the first step the value of $\varepsilon^{(1)} = \varepsilon_r$. $\beta_m{}^{(1)}$ must be obtained using $\varepsilon^{(1)}$ and the fifth network. Then, $\Delta\varphi^{(1)}$, $\varphi'^{(1)}$, and $L^{(1)}$ are calculated using (13), and (14), and the second network. With the input of $L_1 = 13.4$ mm, $L = L^{(1)}$ and the sixth network, $\varepsilon_r^{(2)}$ of the structure with the dimension of 13.4 mm is achieved. This iterative step is continued until the absolute value of $\varepsilon_r^{(n+1)} - \varepsilon_r^{(n)}$ becomes larger than the convergence criteria of α. When the convergence condition is satisfied, the final value of L is assigned. Afterwards L is transformed and L_1 is obtained. With the final values of ε_r and β_m, the target phase applied to GEANN is calculated as follows:

$$\Delta\varphi = \beta_m \times (h - 1.6), \tag{13}$$

$$\varphi' = < S_{12} - \Delta\varphi. \tag{14}$$

In these equations, h is the desired substrate thickness in mm and is entered in the first step. If h is smaller than 1.6 mm (63 mil), $<S_{12}$ that can be obtained from the structure is smaller than the reference state. So, the structure must be designed for a bigger phase and vice versa. Following that, network 3 transforms L_1 into L_2 for the substrate with the thickness of h and permittivity of ε_r.

In Section 3, three samples of FSSs are designed using these design algorithms and error of the design procedure is obtained.

III. NUMERICAL AND EXPERIMENTAL RESULTS

A) Numerical results

In this section, three examples of FSSs are designed using the proposed design algorithm. The first test is an FSS filter with the following input parameters: $f_r = 5.41$ GHz, $\theta = 0^\circ$, and TE polarization on the substrate with $\varepsilon_r = 3.55$ and $h = 0.508$ mm. The second example has the input of $f_o = 2.4$ GHz, $<S_{12} = -75^\circ$, $\theta = 45^\circ$, and the transverse magnetic (TM) polarization on the substrate with $\varepsilon_r = 5$ and $h = 2.54$ mm. Finally, a third test considers the input parameters

https://doi.org/10.1017/S1759078716001045 Published online by Cambridge University Press

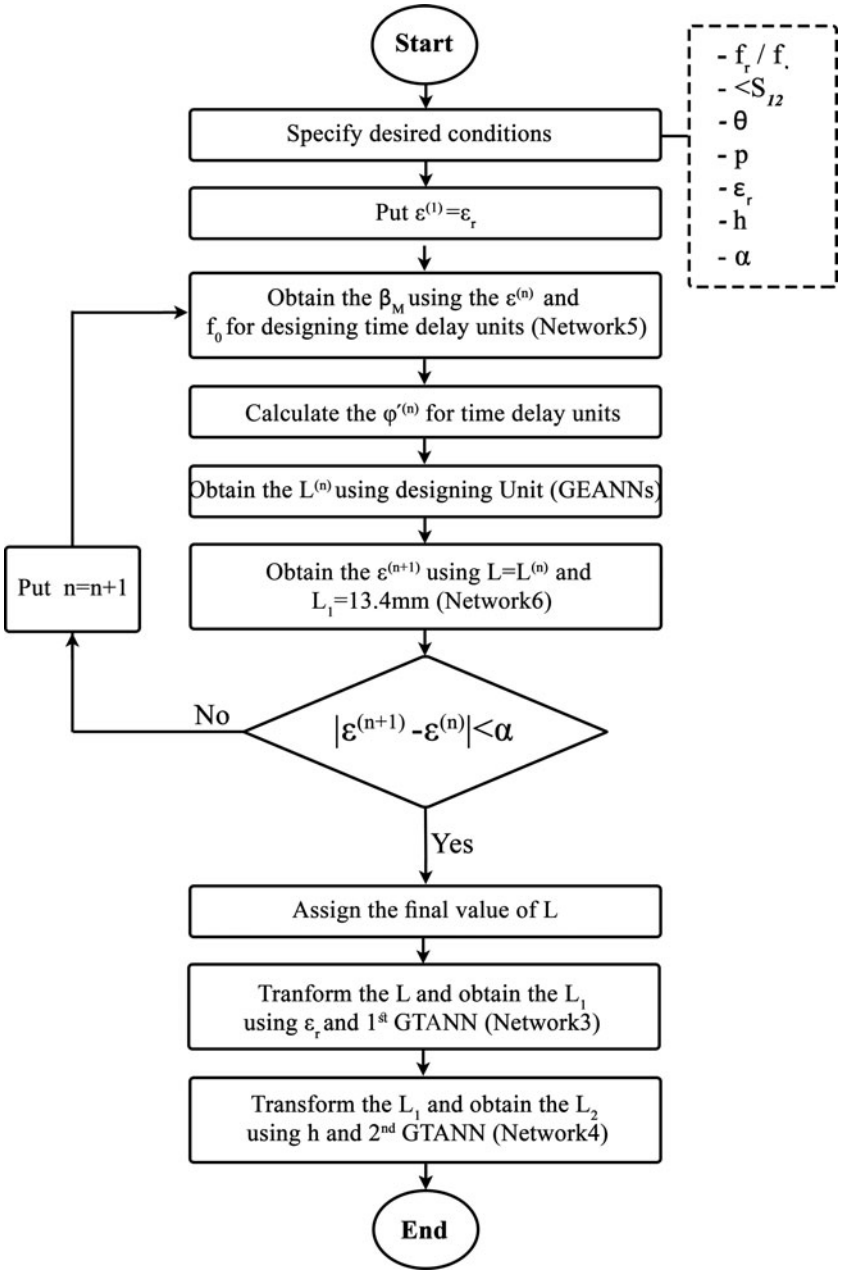

Fig. 7. Design algorithm for standard isotropic substrates.

as $f_o = 3.8$ GHz, $<S_{12} = 70.5^\circ$, $\theta = 30^\circ$, and the TE polarization on the substrate with $\varepsilon_r = 2.2$ and $h = 0.381$ mm. The input conditions and results are shown in Table 1. In tests 2 and 3, convergence criterion of α is 0.1.

As can be seen, the total errors in the design results were less than 2%. FSS samples are developed in $<$250 ms without dealing with any optimization algorithm and its complexities and limitations.

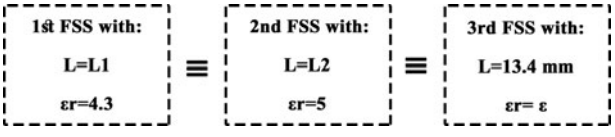

Fig. 8. Equivalent structures for obtaining the correct β_m.

B) Experimental results

The prototype FSS with the specifications of the first test was fabricated. The fabricated FSS, as mentioned in the previous sections, is an array of square loop patches with unit cells having the outer side length of 8.54 mm that are printed on the RO4003 substrate with the thickness of 0.508 mm. The fabricated FSS that is shown in Fig. 9 was tested with the measurement setup demonstrated in Fig. 10. This test setup consisted of two C-band horn antennas (4.9–7.5 GHz) and a spectrum analyzer (Model No Agilent 8563EC). The measured data for the perpendicular incidence are shown in Fig. 11. As can be seen, the resonance frequency was 5.375 GHz that was only shifted by about 40 MHz from the simulations. The depth of resonance was also −37.5 dB, which showed good agreement between the simulation and experimental results.

https://doi.org/10.1017/S1759078716001045 Published online by Cambridge University Press

Table 1. The desired design condition and results of design algorithm for standard isotropic substrates.

		Testl	Test2	Test3
Desired condition	f_o/f_r (GHz)	5.41	2.4	3.8
	$<S_{12}$ (°)	–	−75	70.5
	o (°)	0	45	30
	P	TE	TM	TE
	ε_r	3.55	5	2.2
	h (mm)	0.508	2.54	0.381
Values obtained by ANNs	L (mm)	7.3218	9.5100	10.5
	β_M (°/m)	–	−7.2574	−6.2756
	$\Delta\varphi$ (°)	–	−6.82	−7.65
	φ' (°)	–	−68.18	62.85
	L_1 (mm)	7.8460	8.5823	13.6346
	L_2 (mm)	8.5484	8.5153	15.5653
Values obtained by CST simulations	f_o/f_r with L	5.4104	φ' with L at f_o	−67.35	63.85
	f_o/f_r with L_1	5.4249	φ' with L at f_o	−67.49	62.30
	f_o/f_r with L_2	5.3828	φ' with L at f_o	−75.81	69.49
Error (%)	f_o/f_r with L	0.0073%	φ' with L at f_o	1.2173%	1.591%
	f_o/f_r with L_1	0.2754%	φ' with L at f_o	1.0120%	0.8750%
	f_o/f_r with L_2	0.5027%	φ' with L at f_o	1.08%	1.4326%
Required time for design procedure (ms)		203	209		195

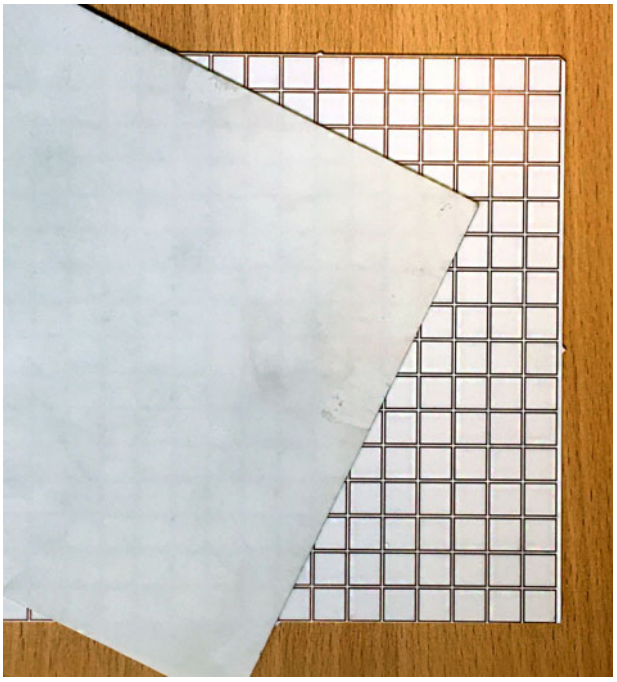

Fig. 9. Fabricated sandwiched FSS with $L = 8.54$ mm on the RO4003 substrate with 0.508 mm thickness.

The errors were mainly because of the fabrication process. Finally, it can be stated that the experimental results as simulation results showed good accuracy of the design algorithm.

IV. MODELING FSS WITH UNIAXIALLY ANISOTROPIC SUBSTRATES

In recent years, considerable efforts have been made to analyze and design FSSs with anisotropic substrates [14–20]. For the first time, in this paper, the efficient design algorithm was provided for developing FSSs with anisotropic materials. In the previous section, designing FSSs on the desired isotropic substrates was thoroughly described. To achieve the design algorithm in this section, the first step is to compare the response of FSS on uniaxial substrates with isotropic ones.

Fig. 10. Test setup for measuring the scattering parameters of FSS.

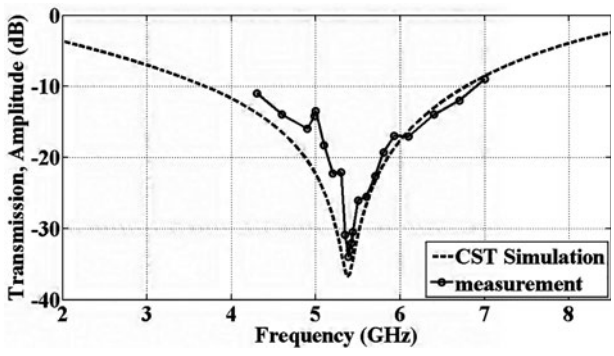

Fig. 11. Comparison between simulated and measured FSS transmission parameter for the perpendicular incident wave.

https://doi.org/10.1017/S1759078716001045 Published online by Cambridge University Press

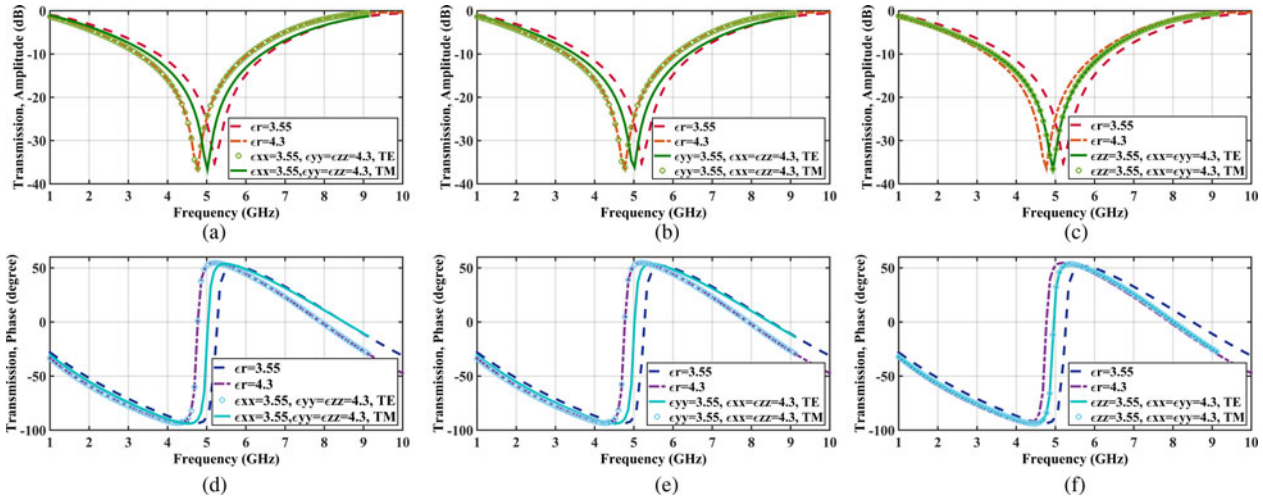

Fig. 12. Frequency responses of square loop with three types of anisotropic substrates: (a) state 1, $|S_{12}|$; (b) state 2, $|S_{12}|$; (c) state 3, $|S_{12}|$; (d) state 1, $<S_{12}$; (f) state 2, $|<S_{12}$; (g) state 3, $<S_{12}$.

The results help find the way of using the aforesaid design method for uniaxial substrates as well. Assume the square loop on the uniaxial substrate with the following permittivity tensor:

$$\varepsilon_r = \begin{bmatrix} \varepsilon_{xx} & 0 & 0 \\ 0 & \varepsilon_{yy} & 0 \\ 0 & 0 & \varepsilon_{zz} \end{bmatrix}. \quad (15)$$

Three states can be supposed for this tensor:

(1) Optical axis that is along x; $\varepsilon_{yy} = \varepsilon_{zz} \neq \varepsilon_{xx}$;
(2) Optical axis that is along y; $\varepsilon_{xx} = \varepsilon_{zz} \neq \varepsilon_{yy}$;
(3) Optical axis that is along z; $\varepsilon_{xx} = \varepsilon_{yy} \neq \varepsilon_{zz}$.

For each state, a sample is simulated and compared with the isotropic ones. Figure 12 depicts the frequency responses of FSS on the anisotropic material for each of these states. As can be seen, in state 1, the TE response of FSS with anisotropic substrate coincides with the response of FSS with an isotropic substrate and the permittivity of ε_{yy}. The TM response is near the response of FSS with an isotropic substrate and the permittivity of the geometric mean of ε_{yy} and ε_{xx}.

It is obvious that the mentioned relation is exchanged between TE and TM modes in state 2. In state 3, both TE and TM polarizations coincide on the geometric mean of isotropic responses. These results are valid for any permittivity between 1.5 and 12.5. For brevity, the results of 3.55 and 4.3 are only mentioned.

With due attention to these rules, two scenarios can be assumed for uniaxial substrates as follows:

- First: FSSs are designed with uniaxial substrates with the optical axis along x or y (parallel to the surface of FSS). In this scenario, the goal is to create the structure with different behaviors against TE and TM polarizations.
- Second: Materials with the optical axis along z (perpendicular to the surface of FSS). In this scenario, the goal is to achieve the frequency response that cannot be produced by standard isotropic substrates and the structure must have the same responses for TE and TM polarizations.

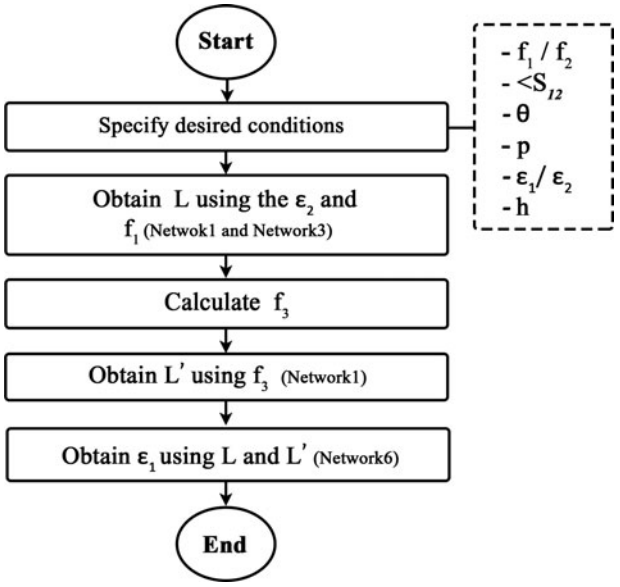

Fig. 13. Design flowchart for the first scenario when input permittivity is ε_2.

Figure 13 shows the design algorithm for the first scenario. In this scenario, one of the permittivities must be determined during the design procedure to control the frequency response of two modes separately. So, only one of the permittivities is taken from the user. For simplicity, it assumed that ε_r along the optical axis is named ε_1 (it can be ε_{yy} or ε_{xx}) and called the other one is called ε_2. The input parameters for this algorithm are similar to the isotropic state except that for each polarization, the specific f_o/f_r is determined by the user. During the design process, first, L is obtained using f_1 and GEANNs. Afterwards position of another polarization is considered the frequency response of FSS on the substrate with the permittivity of the geometrical mean of ε_1 and ε_2. The operational frequency of the structure on an isotropic substrate with ε_2 is determined using (16) and (17).

$$f_2 = \sqrt{f_1 f_3}, \quad (16)$$

https://doi.org/10.1017/S1759078716001045 Published online by Cambridge University Press

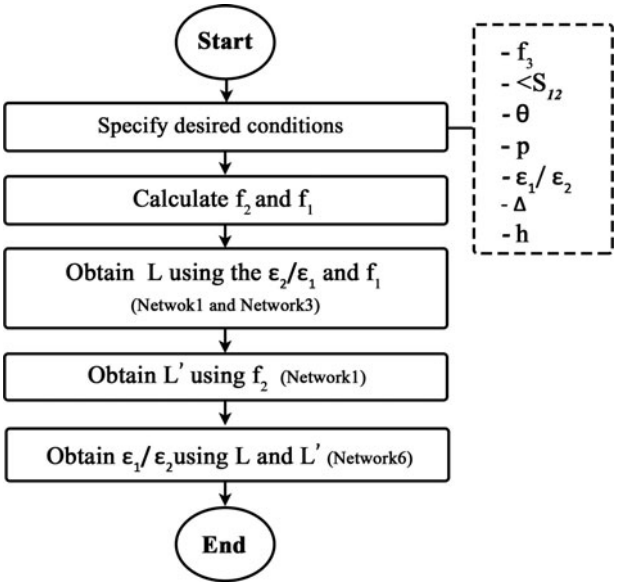

Fig. 14. Design flowchart for the second scenario when input permittivity is ε_1.

Table 2. The desired design condition and results of design algorithm for uniaxial substrates.

		Testl		Test2
Desired conditions	f_{o1}/f_{r1} (GHz)	5.2		5.4
	f_{o2}/f_{r2} (GHz)	4.8		
	θ (°)	0		0
	ε_1	3.55 (ε_{xx})		2.2
	Δ	–		1.1
	h (mm)	1.6		1.6
Values obtained by ANNs	Final length (mm)	9.1582		7.9158
			f_1	5.9400
	f_3 (GHZ)	4.1689		
			f_2	4.9091
	ε_2	2.5352 (ε_{yy})		4.2948
Values obtained by CST simulations	f_{o1}/f_{r1} (GHz)	5.1992		5.3691
	f_{o2}/f_{r2} (GHz)	4.7816		5.378
Error (%)	f_{o1}/f_{r1} (GHz)	0.0153%		0.5722%
	f_{o2}/f_{r2} (GHz)	0.3848%		0.4074%
Required lime for design procedure (ms)		220		210

$$f_3 = \frac{(0.97^* f_2)^2}{f_1}. \tag{17}$$

In (16), f_1 and f_2 are the operational frequencies entered by the user. The correction factor of about 0.97 is added by trial-and-error in order to decrease the amount of error. In the next step, L' is calculated using ε_1, f_3, network 1, and network 3.

Finally, using network 6, L, and L', ε_2 is assigned and the design procedure is completed.

Scenario 2 that is shown in Fig. 14 requires the position of the operational frequency for both modes. In this scenario, like the algorithm of the standard substrates, only one f_o/f_r and one permittivity (ε_2 or ε_1) are determined by the user. It is supposed that this frequency is the geometrical mean of ε_2 and ε_1. In addition to these inputs, one other parameter is specified to determine f_1 and f_2 from f_3, which is called Δ. Using these parameters, f_1 and f_2 are calculated as follows:

$$f_1 = 0.95 \times \Delta \times f_3, \tag{18}$$

$$f_2 = \frac{0.95 \times f_3}{\Delta}. \tag{19}$$

In the next step, first, L is obtained using f_1, ε_1, networks 1, and network 3. Then, L' is obtained using f_2 using GEANNs. Finally, ε_2 is determined by network 6.

Two design samples are provided in Table 2. The errors and required time for completing the design algorithm approximate each other. Results show the high ability of GTANNs and the proposed algorithms for designing FSSs on uniaxial substrates.

V. CONCLUSION

EGA method has been presented as a new approach in training ANNs for designing electromagnetic surfaces. Various parameters exist that influence the frequency response of FSSs. EGA offers the chance to remove some of these parameters from the inputs of primary networks, but considers them in the design procedure. The time savings of the EGA are more pronounced when this method can reduce the size of the pre-simulations by about 98%. Using this method, GTANNs are trained. The input of these networks is the length of the structure with the reference substrate, permittivity, and thickness of the substrate. The output of the design algorithm is the transformed dimension that have the same frequency response on the new substrate.

GTANNs are employed for designing FSSs on the standard isotropic substrates. In addition, uniaxial substrates can be designed for obtaining the desired behavior of FSS for each polarization by GTANNs. GTANNs do all of the operations mentioned above without any optimization algorithms. Design procedures based on GTANNs have good accuracy and versatility.

The proposed design algorithms were used for designing three samples of FSSs on isotropic substrates and two samples of FSSs on uniaxial substrates. Errors were estimated and it was observed that this design algorithm could solve the inverse problem of FSS design with the errors of $<2\%$. Also, the required time for finishing the design process was <250 ms. In the experimental test, the measured data for the fabricated structure also showed the accuracy of these design procedure.

The primary advantages of using GTANNs were the flexibility of networks under various specifications of the substrates, high accuracy and versatility of networks, fast designing process, fabrication facility of the designed structures, and ability to design on uniaxial substrates for the first time.

https://doi.org/10.1017/S1759078716001045 Published online by Cambridge University Press

ACKNOWLEDGEMENTS

We thank our colleagues from Iran University of science and Technology (IUST) who provided insight and expertise that greatly assisted the research. We would like to express our sincere appreciation and gratitude to Mr. Ali Mohtadi for his guidance during my research. We thank Mr. Mohammad Kiani for assistance with writing paper methods, and Mr. Hamid Rajabalipanah for comments that greatly improved the manuscript. We would also like to show our gratitude to the Mr. Mohammad Hossein Fakheri and Mr. Mohammad Baharian for sharing their pearls of wisdom with us during the course of this research, and we thank 3 "anonymous" reviewers for their so-called insights. We are also immensely grateful to all of the members of the Applied Electromagnetics Lab for their comments on an earlier version of the manuscript.

REFERENCES

[1] Bayatpur, F.: Metamaterial-Inspired Frequency-Selective Surfaces, Diss., the University of Michigan, Ann Arbor, 2009.

[2] Kern, D.J.; Werner, D.H.; Lisovich, M.: Metaferrites: using electromagnetic bandgap structures to synthesize metamaterial ferrites. IEEE Trans. Antennas Propag., **53** (2005), 1382–1389.

[3] Monorchio, A.; Manara, G.: Synthesis of artificial magnetic conductors by using multilayered frequency selective surfaces. IEEE Antennas Wireless Propag. Lett., **1** (2002), 196–199.

[4] Kiani, G.I.; Ford, K.L.; Esselle, K.P.; Wei, A.R.; Panagamuwa, C.J.: Oblique incidence performance of a novel frequency selective surface absorber. IEEE Trans. Antennas Propag., **55** (2007), 2931–2934.

[5] Munk, B.: Frequency Selective Surfaces: Theory and Design, Wiley, New York, 2000.

[6] Wu, T.: Frequency Selective Surface and Grid Array, Wiley, New York, 1995.

[7] Chandrika, S.; Madhu, A.R.; Mahesh, A.; Pillai, A.C.R.: FSS radomes for antenna RCS reduction. Int. J. Adv. Eng. Technol., **6** (2013), 464–1473.

[8] Euler, M.; Fusco, V.; Cahill, R.; Dickie, R.: Comparison of frequency selective screen-based linear to circular split-ring polarization converters. IET Microw. Antennas Propag., **4** (2010), 1764–1772.

[9] Ma, B.; Xia, M.; Yan, L.: Design of a K-band reflectarray antenna using double square ring elements. Microw. Opt. Technol. Lett., **54** (2012), 394–398.

[10] Abu, M.; Rahim, M.K.A.: Single-band and dual-band artificial magnetic conductor ground planes for multiband dipole antenna. Radio Eng., **21** (2012), 999–1006.

[11] Foroozesh, A.; Shafai, L.: Investigation into the effects of the patch-type FSS superstrate on the high-gain cavity resonance antenna design. IEEE Trans. Antennas Propag., **58** (2010), 258–270.

[12] Callaghan, P.; Parker, E.A.; Langley, R.J.: Influence of supporting dielectric layers on the transmission properties of frequency selective surfaces. IEE Proc. H, **138** (1991), 448–454.

[13] Zhang, H., Lu, J., Sun, G.; Xiao, H.: Influence of substrate tolerances on transmission characteristics of frequency-selective surfaces. Chin. Opt. Lett., **6** (2008), 54–56.

[14] Campos, A.L.P.S.; D'Assunção, A.G.; De Melo, M.A.B.: Frequency selective surfaces with anisotropic dielectric superstrates. Int. J. Infrared Millim. Waves, **21** (2000), 461–475.

[15] Campos, A.L.P.S.; D'Assunção, A.G.; De Melo, M.A.B.: Scattering parameters of FSS on anisotropic layers at millimeter wave frequencies. Int. J. Infrared Millim. Waves, **23** (2002), 123–133.

[16] Campos, A.L.P.S.; D'Assunção, A.G.; de Mendonça, L.M.: Scattering parameters of FSS on the substrate for TE and TM excitation. IEEE Trans. Microw. Theory Technol., **50** (2002), 72–76.

[17] Boufrioua, A.; Benghalia, A.: Effects of the resistive patch and the uniaxial anisotropic substrate on the resonance frequency and the scattering radar cross section of rectangular microstrip antenna. Aerosp. Sci. Technol., **10** (2006), 217–221.

[18] Lin, B.; Liu, S.; Yuan, N.: Analysis of frequency selective surfaces on electrically and mechanically anisotropic substrates. IEEE Trans. Antennas Propag., **54** (2006), 674–680.

[19] Campos, A.L.P.S.; D'Assunção, A.G.: Frequency selective surfaces on iso/anisotropic substrates with dielectric losses. Microw. Opt. Technol. Lett., **49** (2007), 1041–1044.

[20] Fallahi, A.; Mishrikey, M.; Hafner, C.; Vahldieck, R.: Analysis of multilayer frequency selective surfaces on periodic and anisotropic substrates. Metamaterials, **3** (2009), 63–74.

[21] Langley, R.J.; Parker, E.A.: Equivalent circuit model for arrays of square loops. Electron. Lett., **18** (1982), 294–296.

[22] Lee, C.K.; Langley, R.J.: Equivalent circuit models for frequency selective surfaces at oblique angles of incidence. IEE Proc. H, **132** (1985), 395–399.

[23] Kent, E.; Doken, B.; Kartal, M.: A new equivalent circuit based FSS design method by using a genetic algorithm, in Int. Conf. on Engineering Optimization, Lisbon, 2010, 1–4.

[24] Marcuvitz, N.: Waveguide Handbook, McGraw-Hill, New York, 1951.

[25] Gunes, F.; Demirel, S.; Nesil, S.: A novel design approach to x-band Minkowski reflectarray antenna using the full-wave em simulation-based complete neural model with a hybrid ga-nm algorithm. Radio Eng., **23** (2014), 144–153.

[26] Silva, P.H.F.; Campos, A.L.P.S.: Fast and accurate modeling of frequency selective surfaces using a new modular neural network configuration of multilayer perceptrons. IET Microw. Antenna Propag., **2** (5) (2008), 503–511.

[27] da Silva, M.R.; Nobrega, C.d.L.; Silva, P.H.d.F.; D'Assunção, A.G.: Optimization of FSS with Sierpinski island fractal elements using population-based search algorithms and MLP neural network. Microw. Opt. Technol. Lett., **56** (2014), 827–831.

Sara Moinzad was born in Tehran, Iran on July 14, 1989. She received her B.Sc. degree in Electrical Engineering from Iran University of Science and Technology in 2013. She is currently working toward her M.S. in Iran University of Science and Technology. Her research interests include frequency selective surface; computer aided design methods, metamaterials, complex electromagnetic surfaces and realization methods, artificial neural networks and computational electromagnetics.

https://doi.org/10.1017/S1759078716001045 Published online by Cambridge University Press

Ali Abdolali was born in Tehran, Iran, on May 3, 1974. He received B.Sc. degree from the University of Tehran, and M.S. degree from the University of Tarbiat Modares, Tehran, and the Ph.D. degree from the Iran University of Science and Technology (IUST), Tehran, all in electrical engineering, in 1998, 2000, and 2010, respectively. In 2010, he joined the Department of Electrical Engineering, Iran University of Science and Technology, Tehran, Iran, where he is an Assistant Professor of Electromagnetic Engineering. His research interests include electromagnetic wave scattering, radar cross section (RCS) & RCSR, radar absorbing materials (RAM), cloaking, metamaterials, wave propagation in complex media (anisotropic, inhomogeneous, dispersive media), frequency selective surfaces (FSS), and bioelectromagnetism (BEM). He has authored or coauthored over 100 papers in international journals & conferences.

Bagher Noorbakhsh was born in golpayegan, Iran on January 30 1981. He received B.Sc. degree from Air University of Sattari, and M.S. degree from the University of Khaje Nasir Toosi (KNTU) Tehran, all in Electrical Engineering, in 2003, 2007, respectively. He is currently working toward his Ph.D. in Iran University of Science and Technology (IUST), Tehran. His research interests include radar absorbing materials (RAM), radar cross section (RCS) & RCSR, electromagnetic wave scattering, radar technology, and wave propagation in complex media.

https://doi.org/10.1017/S1759078716001045 Published online by Cambridge University Press